

Manuscript Number: JCR-D-16-00840

Title: Selective delivery of doxorubicin by novel stimuli-sensitive nano-ferritins overcomes tumor refractoriness

Article Type: Research paper

Keywords: protein-cage nanocarrier; ferritin; PASylation; nuclear localization; drug-delivery; pancreatic cancer

Corresponding Author: Dr. Pierpaolo Ceci, PhD

Corresponding Author's Institution: National Research Council of Italy, CNR

First Author: Giulio Fracasso

Order of Authors: Giulio Fracasso; Elisabetta Falvo; Gianni Colotti; Francesco Fazi; Tiziano Ingegnere ; Adriana Amalfitano ; Giovanni B Doglietto ; Sergio Alfieri; Alberto Boffi; Veronica Morea; Giamaica Conti ; Elisa Tremante; Patrizio Giacomini; Alessandro Arcovito ; Pierpaolo Ceci, PhD

Abstract: Human ferritin heavy chain (HfT) has been demonstrated to possess considerable potential for targeted delivery of drugs and diagnostic agents to cancer cells. Here, we report the development of a novel HfT-based genetic construct (HfT-MP-PAS) containing a short peptide linker (MP) between each HfT subunit and an outer shielding polypeptide sequence rich in proline (P), serine (S) and alanine (A) residues (PAS). The peptide linker contains a matrix-metalloproteinases (MMPs) cleavage site that permits the protective PAS shield to be removed by tumor-driven proteolytic cleavage within the tumor microenvironment. For the first time HfT-MP-PAS ability to deliver doxorubicin to cancer cells, subcellular localization, and therapeutic efficacy on a xenogeneic mouse model of a highly refractory to conventional chemotherapeutics type of cancer were evaluated. HfT-MP-PAS-DOXO performance was compared with the novel albumin-based drug delivery system INNO-206, currently in phase III clinical trials. The results of this work provide solid evidence indicating that the stimuli-sensitive, long-circulating HfT-MP-PAS nanocarriers described herein have the potential to be exploited in cancer therapy.

Suggested Reviewers: Oksana Kasyutich
Faculty of Engineering, University of Bristol (UK)
Oksana.kasyutich@bristol.ac.uk

Reviewer expertise: Nanotechnology, Biomaterial characterization, protein-based nanosystems synthesis

Francesco Angelucci
Dep. of Life, Health and Environmental Sciences, University of L'Aquila,
francesco.angelucci@univaq.it
Reviewer expertise: Protein-based nanomaterials synthesis and Protein engineering

Jeroen J.L.M Cornelissen
Biomolecular Nanotechnology, University of Twente
J.J.L.M.Cornelissen@tnw.utwente.nl
Reviewer expertise: Biomolecular Nanotechnology, Bio-inspired materials,
biopolymers

Mauri Kostianen@aalto.fi
Department of Biotechnology and Chemical Technology, Aalto University,
Finland
mauri.kostianen@aalto.fi
Reviewer expertise: Biohybrid Materials and Bio-inspired materials,
protein-cages synthesis and characterization, smart supramolecular
assemblies

Giuliano Bellapadrone
Department of Materials and Interfaces., Weizmann Institute of Science
giuliano.bellapadrone@weizmann.ac.il
Biomaterials and protein-cages synthesis and characterization, ferritin-
based systems.

Wijnand Helfrich
Faculty of Medical Sciences, Department of Surgery , University Medical
Center Groningen, The Netherlands
w.helfrich@umcg.nl
Reviewer expertise: Oncology, targeted strategies in cancer, cancer
therapeutics, mouse models

Michele Milella
IFO- Istituto Nazionale Tumori Regina Elena
milella@ifio.it
Expert in the field of cancer diagnosis and treatment, especially
pancreatic cancer. Dr. Milella' research group is involved on preclinical
and clinical development of new targeted constructs.

Dear Editor,

we are submitting to your attention the original article “*Selective delivery of doxorubicin by novel stimuli-sensitive nano-ferritins overcomes tumor refractoriness*”, which we would like to be considered for publication in Journal of Controlled Release.

The manuscript reports the design, development and anti-cancer *in vitro* and *in vivo* properties of a novel protein-based nanocarrier for chemotherapeutic agents. The therapeutic efficacy of our doxorubicin-loaded nanocarrier in a mouse model bearing xenogenic human pancreatic tumor is striking, since it is even superior to that of the novel doxorubicin prodrug formulation INNO-206 (human albumin-based), which is currently undergoing phase III clinical trials. This result is even more remarkable in that the chosen tumor model is extremely refractory to conventional chemotherapeutic drugs such as doxorubicin, indicating that the implemented nanocarrier successively delivers the drug to its target destination. Interestingly, the higher *in vivo* efficacy of our nanosystems could also be ascribable to the massive delivery into the cell nucleus as observed in the confocal microscopy studies.

The nanocarrier is based on the physiological human protein ferritin (HFt), which is endowed with a number of favourable characteristics, including: *in vitro* and *in plasma* solubility; capacity to stably (months/years) encapsulate different types of drugs; and ability to selectively bind to and be imported by cancer cells. This selectivity is due to the fact that the transferrin receptor (TfR1-CD71), with which HFt interacts, is expressed at significantly higher levels by tumors with respect to normal cells. In this work, to further enhance tumor selectivity with respect to normal tissues, we have engineered HFt to endow it with: i) a peptide-based polymeric shell, effectively masking HFt from TfR1-CD71 in normal tissues, which are therefore more spared from doxorubicin accumulation; and ii) a tag sequence, which allows the polymeric shield to be selectively removed in the presence of stimuli peculiar to the tumor microenvironment (matrix-metalloproteinases, MMP 2/9), such that doxorubicin-loaded HFt nanocarriers can be incorporated in cancer cells *via* TfR1. As an additional useful feature for therapeutic applications, the nanocarrier derives from a fully genetic construct that can be expressed as a single protein product with no additional coupling and/or separation steps required.

Altogether, the results presented in this work provide strong evidence that the new HFt-based nanocarrier here presented may be successfully exploited to deliver anti-tumor payloads in cancer therapy.

For all the above, we believe that this manuscript might be of interest for the readers of Journal of controlled Release.

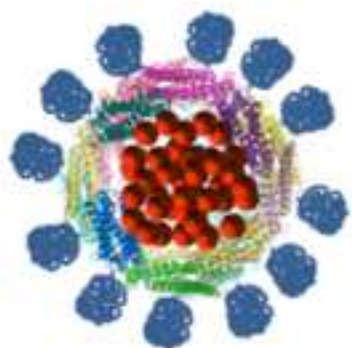
Thanking you in advance for your kind attention,




Sincerely,

On behalf of all the authors,

Pierpaolo Ceci and Alessandro Arcovito

Hft-MP-PAS40-DOXO

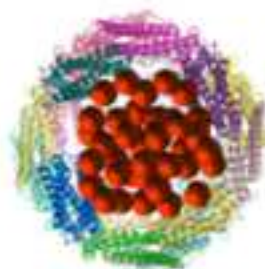


-  Matrix metallo-protease (MMP)-cleavable linker
-  Shielding moiety (polypeptide-based)
-  Doxorubicin

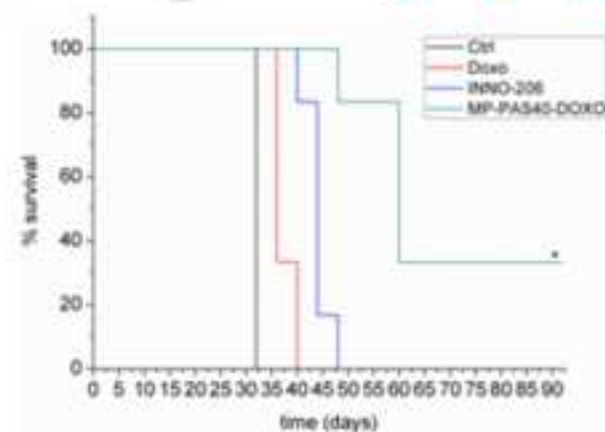
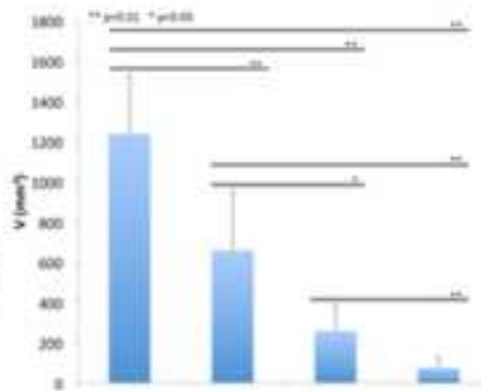
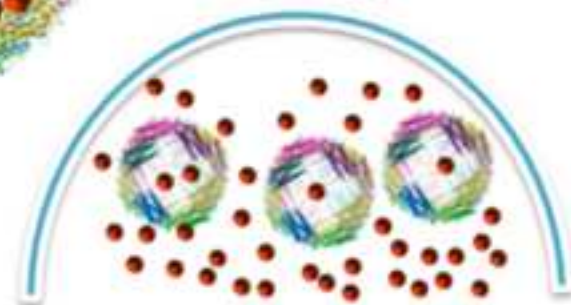
Selective release of the shielding



MMPs-mediated cleavage in tumor microenvironment



Nuclear Drug release



Selective delivery of doxorubicin by novel stimuli-sensitive nano-ferritins overcomes tumor refractoriness

Giulio Fracasso ^{a,1}, Elisabetta Falvo ^{b,1}, Gianni Colotti ^b, Francesco Fazi ^c, Tiziano Ingegnere ^d, Adriana Amalfitano ^e, Giovanni Battista Doglietto ^f, Sergio Alfieri ^f, Alberto Boffi ^{b,g,h}, Veronica Morea ^b, Giamaica Conti ⁱ, Elisa Tremante ^d, Patrizio Giacomini ^d, Alessandro Arcovito ^{e,*}, and Pierpaolo Ceci ^{b,*}

a Department of Medicine, University of Verona, 37134 Verona, Italy

b Institute of Molecular Biology and Pathology, CNR – National Research Council of Italy, 00185 Rome, Italy

c Department of Anatomical, Histological, Forensic & Orthopedic Sciences, Section of Histology & Medical Embryology, “Sapienza” University, 00161 Rome, Italy

d Oncogenomics and Epigenetics, Regina Elena National Cancer Institute, 00144 Rome, Italy

e Institute of Biochemistry and Clinical Biochemistry, Catholic University, 00168 Rome, Italy

f Digestive Surgery Division, Department of Surgical Sciences, Catholic University, 00168 Rome, Italy

g Department of Biochemical Sciences “A. Rossi-Fanelli”, “Sapienza” University, 00185 Rome, Italy

h Center for Life Nano Science at “Sapienza” University, Italian Institute of Technology (IIT), 00161 Rome, Italy

i Department of Neurological and Movement Sciences, University of Verona, 37134 Verona, Italy

* Corresponding authors:

e-mail address: pierpaolo.ceci@cnr.it (P. Ceci); alessandro.arcovito@unicatt.it (A. Arcovito)

¹ The authors contributed equally to this work

Keywords: protein-cage nanocarrier; ferritin; PASylation; nuclear localization; drug-delivery; pancreatic cancer

ABSTRACT. Human ferritin heavy chain (HFt) has been demonstrated to possess considerable potential for targeted delivery of drugs and diagnostic agents to cancer cells. Here, we report the development of a novel HFt-based genetic construct (HFt-MP-PAS) containing a short peptide linker (MP) between each HFt subunit and an outer shielding polypeptide sequence rich in proline (P), serine (S) and alanine (A) residues (PAS). The peptide linker contains a matrix-metalloproteinases (MMPs) cleavage site that permits the protective PAS shield to be removed by tumor-driven proteolytic cleavage within the tumor microenvironment. For the first time HFt-MP-PAS ability to deliver doxorubicin to cancer cells, subcellular localization, and therapeutic efficacy on a xenogeneic mouse model of a highly refractory to conventional chemotherapeutics type of cancer were evaluated. HFt-MP-PAS-DOXO performance was compared with the novel albumin-based drug delivery system INNO-206, currently in phase III clinical trials. The results of this work provide solid evidence indicating that the stimuli-sensitive, long-circulating HFt-MP-PAS nanocarriers described herein have the potential to be exploited in cancer therapy.

1. Introduction

Ferritin is a highly symmetrical multimeric protein. It consists of 24 heavy and light chain subunits that self-assemble into a shell-like sphere, with external and internal diameters of 12 and 8 nm, respectively, which encloses a hollow cavity for iron storage. Recombinant ferritins made of 24 heavy chains (HFt) are endowed with considerable potential for the targeted delivery of drugs and diagnostic agents to cancer cells.^[1-15] HFt numerous advantageous characteristics include: biosafety; water and blood solubility; amenability to multi-functionalization; and intrinsic ability to bind tumor cells in an effective and selective way.

HFt has a remarkable capacity to entrap different types of drugs, and several groups including ours have reported that ferritins are effective templates for loading, in their internal cavity, imaging agents for magnetic resonance imaging (MRI), positron emission tomography (PET), organic molecules and drugs.^[1-3, 16-21]

Importantly, HFt is one of the few nanoparticles (NPs) that are intrinsically able to effectively and selectively bind tumor cells thanks to its interaction with, and internalization via, transferrin receptor 1 (TfR1,CD71).[22] TfR1 is one of the most attractive cancer therapy targets, since it is up-regulated at the surface of many types of cancers. Tumors express up to 100 times higher levels of TfR1 than healthy cells, and actively internalize the HFt:TfR1 ligand-receptor complex, to accumulate the large amounts of iron required for unrestrained cell growth.[3] As a consequence,

cancer cells addiction to iron is an attractive basis to selectively deliver HFt carrying toxic payloads to cancer lesions.

Very recently, to increase both the *in vivo* half-life of natural HFt and the stability of HFt-drug complexes, we have developed novel HFt-based constructs where each HFt subunit is genetically fused to a PAS polypeptide sequence, i.e., a sequence rich in proline (P), alanine (A) and serine (S) residues.[23] Two HFt-PAS constructs, containing PAS polymers with lengths of 40 and 75 residues, had dramatically increased stability (with no drug-leakage observed for months/years) and considerably longer *in vivo* circulation time with respect to wild-type HFt. Remarkably, both constructs were able to encapsulate three times more doxorubicin (DOXO) than wild-type HFt in their internal cavity and pharmacokinetic profiles were superior either to the wild-type HFt and to the albumin-conjugated DOXO formulation INNO-206.[23]

In the present study, we describe two novel HFt-based nanocarriers, aimed at further increasing the tumor selectivity with respect to the previously reported HFt-PAS systems. In the new constructs, 40 or 75 residue long PAS polypeptides are genetically linked to HFt subunits by peptides containing cleavage sites for matrix metalloproteinases involved in tumor angiogenesis, invasion, and metastasis (Fig. 1).[24] By surface plasmon resonance, biochemical methods, flow cytometry, confocal microscopy and *in vitro* cell proliferation assays we show that the PAS polypeptides are shaved off both HFt-MP-PAS40-DOXO and HFt-MP-PAS75-DOXO nanocarriers by metalloproteinases expressed by tumor cells. Thus, PAS acts as a temporary shield, hampering the interaction of drug-loaded HFt with TfR1 expressed by normal cells, albeit at low levels; once the nanocarrier reaches the tumor microenvironment, the PAS shield is removed by specific stimuli and the unmasked HFt is free to interact with, and be internalized by, the overexpressed TfR1.

HFt-MP-PAS40-DOXO in particular has antineoplastic properties towards human sarcoma cells, human pancreas adenocarcinoma cells, and xenotransplants. As argued below, these features compare favourably with naked DOXO and state-of-art drug delivery systems such as INNO-206. Thus, HFt-MP-PAS40-DOXO candidates as a potential first-in-class nanocarrier for conditional, stimuli-sensitive cancer therapy. Moreover our data demonstrate that HFt-MP-PAS40 system could be also considered a suitable platform for the specific delivery of different drugs to cancer sites.

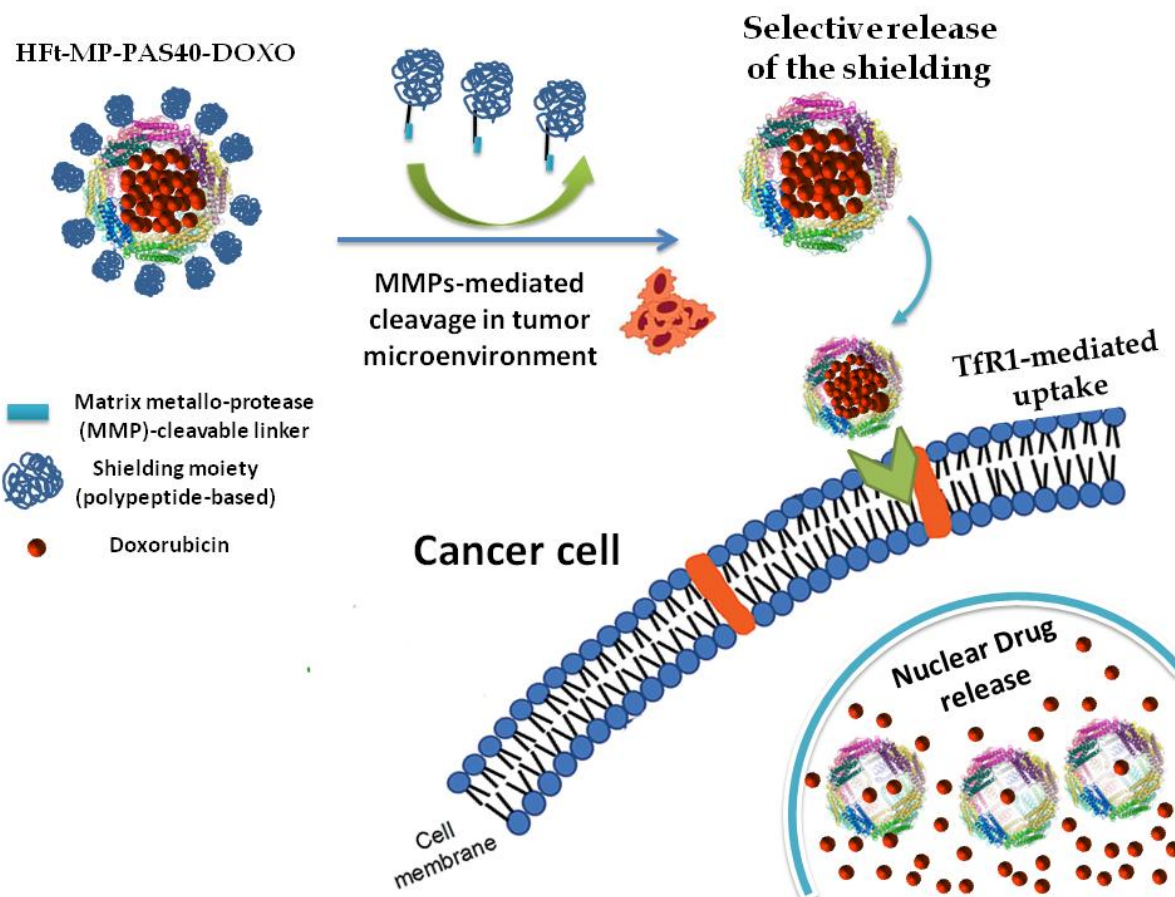


Fig. 1. Rationale for the construction of stimuli-sensitive HFt-based NPs. After HFt-NP accumulation at the tumor level, PAS sequences are selectively removed by MMP2/9 that are over-expressed in the tumor microenvironment. The removal of the PAS shield enhances TfR1 mediate cell binding and internalization, and the delivery of DOXO molecules to the cancer cell nucleus.

2. Material and methods

2.1. Cloning, overexpression and purification of HFt-based constructs

The novel HFt-MP-PAS constructs, named HFt-MP-PAS40 and HFt-MP-PAS75, are identical to the previously described HFt-PAS40 and HFt-PAS75 except for the interposition of the PLGLAG sequence, which is recognized as a proteolytic cleavage site by matrix metallo-proteinases such as MMP-2 and MMP-9, between HFt and the 40 (PAS40) or 75 (PAS75) residue

long PAS sequences. The constructs were codon-optimized for high-level expression in *Escherichia coli*, assembled by whole-gene synthesis at GENEART AG (Regensburg, Germany), cloned in the expression vector pET-11a, introduced into *E. coli* BL21(DE3) and finally expressed and purified as previously described.[23] The purity of all the preparations was assessed by SDS-PAGE on 15% acrylamide gels stained with Coomassie brilliant blue. Protein concentrations were determined spectrophotometrically at 280 nm, using a molar extinction coefficient (on a 24-mer basis) of $4.56 \times 10^5 \text{ M}^{-1} \text{ cm}^{-1}$ (ProtParam software, <http://www.expasy.org>).

2.2. Size exclusion chromatography (SEC) analyses

SEC experiments were performed using a Superose 6 gel-filtration column equilibrated with phosphate buffered saline (PBS) at pH 7.4. All SEC experiments traces were analyzed with Origin 8.0 (Originlab Corporation, Northampton, MA).

2.3. Surface plasmon resonance (SPR)

The interactions between the immobilized N-terminal His-tagged transferrin receptor TfR1 (ligand) and Hft-based constructs (analytes) were measured by surface plasmon resonance (SPR) technique on a Biacore X100 instrument (Biacore, Uppsala, Sweden). TfR1 was immobilized on a Sensor Chip nitrilotriacetic acid (NTA). The NTA group is activated by nickel ions (Ni^{2+}) to selectively bind histidine-tagged TfR1, which can be stripped from the surface by removing the nickel ions with EDTA or other chemicals (regeneration phase). The capturing procedure on the biosensor surface was performed according to the manufacturer's instructions. After a scouting step, the optimal experimental setup was determined: TfR1 was injected at 25 $\mu\text{g/ml}$ for 60 s, followed by 10 s stabilization; this determined a 200 Response Unit (RU) value for the bound ligand (R_L). Analyte concentrations were in the range 300-15 $\mu\text{g/ml}$. Specific values for the different derivatives are reported in figure captions.

The sensor chip surface was regenerated using fresh histidine-tagged protein at every cycle of the assay. The SPR assay was performed at 25°C, at flow rate = 30 $\mu\text{l/min}$; the association and dissociation phases were monitored for 180 and 600 s, respectively. Analytes were dissolved in degassed 10 mM PBS buffer at pH 7.4. To regenerate the chip, complete dissociation of the complexes was achieved by the addition of 10 mM HEPES, 150 mM NaCl, 350 mM EDTA and 0.005% (vol/vol) surfactant P20 (pH 8.3) for 30 s before each new cycle. The k_{on} and k_{off} rates as

well as the dissociation constant (K_D) were estimated using the Biacore X100 evaluation software according to a 1:1 binding model.

2.4. Doxorubicin encapsulation in HFt-based nanocarriers

The chemotherapeutic agent doxorubicin (DOXO) was encapsulated using the previously reported HFt disassembly/reassembly procedure.[23]

2.5. Removal of PAS polypeptides from HFt-based nanocarriers in the presence of MMP2/9 proteinases

To assess enzymatic cleavage of MMP-sensitive conjugates, HFt-MP-PAS40 and HFt-MP-PAS75 cleavage was studied in the presence of MMP-2/9. HFt-MP-PAS solutions were mixed with collagenase IV (containing MMP2 and 9) and incubated at 37°C for two hours. Samples were then analyzed by SEC experiments using a Superose 6 gel-filtration column equilibrated with PBS at pH 7.4, and by SDS-PAGE gel chromatography.

2.6. Cell-binding of HFt-based NPs

Fluorescence Activated Cell Sorting (FACS) and confocal microscopy experiments were carried out after incubation of human fibrosarcoma HT1080 (ATCC, Manassas, VA, USA) and human pancreatic PaCa-44 cells (kindly provided by prof. A. Scarpa, Department of Diagnostics and Public Health University of Verona, Italy) with 0.15 mg/ml (in protein 24-mer) of DOXO-containing HFt-based NPs. To assess PAS removal contribution to cell binding, NPs lacking (HFt-PAS-DOXO) or containing (HFt-MP-PAS-DOXO) the MMP cleavage site were incubated at 4°C and 37°C for 1 hour. Cells (3.5×10^5) were grown in a 6-well plate, incubated at 37°C with 2 ml culture medium (Eagle's Minimum Essential Medium + 10% fetal bovine serum) and fluorescent compounds; at the end of the incubation after a washing step cells were detached by Trypsin-EDTA solution and finally events were collected for each sample with flow cytometer (CyAN ADP; Dako Italia S.p.a., Milan, Italy) using the Summit 4.3 software (Beckman Coulter) for data acquisition and analysis.

2.7. Cell-localization of HFt-based nanocarriers

In confocal microscopy experiments, cells, grown on round glass slides, were treated as described for the cell-binding assays and then fixed in 4% formaldehyde in PBS. After washing

with PBS, slides were mounted with Vectashield (Vector Labs, Burlingame, CA, USA). Cells were examined using a Leica TCS SP2 fluorescence confocal microscope (Leica Microsystems, Wetzlar, Germany) and an excitation wavelength of 488 nm (argon laser). Photomicrographs were acquired with the LAS AF Software (Leica Microsystems).

2.8. Antiproliferative effects of HFt-based nanocarriers *in vitro*

Human fibrosarcoma HT1080 and PaCa44 human pancreatic tumor cells were grown in Eagle's Minimum Essential Medium or RPMI 1640 medium respectively and added with 2 mM glutamine, 10% of FBS and antibiotics. Cancer cells (5×10^3) were seeded one day before the assay in 90 μ L of complete medium in 96 well culture microplates. The following day, cells were incubated in triplicate with 10 μ L of serial dilutions of free DOXO or HFt-MP-PAS-DOXO. After 48 hours the supernatant was removed and cells were washed and finally resuspended in complete RPMI medium. 93 hours after the start of cell incubation with free DOXO or HFt-MP-PAS-DOXO, the medium was replaced with fresh medium w/o phenol red supplemented with XTT (2,3-Bis-(2-Methoxy-4-Nitro-5-Sulfophenyl)-2H-Tetrazolium-5-Carboxanilide) reagent (Sigma-Aldrich, St Louis, MO, USA), according to the manufacturer's instructions. Finally, after 3 hours incubation at 37°C cell viability was measured at 450 nm by a microplate reader (VERSAmax, Molecular Devices, Sunnyvale, CA, USA). The percentage of cell viability was estimated by analyzing the values obtained from cells treated with free DOXO or HFt-MP-PAS-DOXO with respect to mock treated cells. To compare free DOXO and HFt-MP-PAS-DOXO toxicity we evaluated the IC_{50} , i.e., the compound concentration needed to decrease cell viability by 50%.

2.9. Therapeutic evaluation of HFt-based NPs *in vivo*

Five week old female CD1 nude mice (Charles River Laboratories, Lecco, Italy) were injected subcutaneously (i.e., right flank) with 4×10^6 PaCa-44 cells resuspended in 200 μ L of RPMI 1640 medium plus 1% BSA. When tumors had reached a volume of about 100 mm³, mice were randomized in groups of six animals and injected i.v. with 200 μ L of physiological saline, DOXO, INNO-206, HFt-MP-PAS40-DOXO or HFt-MP-PAS75-DOXO. Doses of all injected compounds were normalized to 5 mg/Kg of DOXO. Mice were injected twice a week for two weeks; tumor volume was measured twice a week with a digital caliper and mouse weight was monitored. 24 days after tumor cell injection, when the tumor of mock-treated mice had reached a volume ≥ 900 mm³, animals were sacrificed and tumors were removed, measured and weighted. In the *in vivo*

assay evaluating the overall survival of mice after our i.v. treatments, animals were undergone the same procedures described above and sacrificed when tumors had reached a volume $\geq 900 \text{ mm}^3$. Data were indicated as the mean \pm SD. Student's t test was used to determine statistically significant differences between two treatment groups. All P values less than 0.05 were considered statistically significant.

Animal studies were performed according to a protocol approved by the Institutional Animal Care and Use Committee of University of Verona and authorized by the Italian Ministry of Health (Protocol no. 128/2014-B), and in accordance with the principles laid down in the European Community Council Directives.

3. Results and discussion

3.1. Surface plasmon resonance (SPR)

HFt-PAS40 and HFt-PAS75 constructs were used in a preliminary surface plasmon resonance (SPR) experiment (see below).

HFt-PAS40 and HFt-PAS75 were recently produced by our group and shown to efficiently encapsulate doxorubicin, be highly stable in vitro and in the bloodstream, and have superior pharmacokinetic profiles compared both to wild-type HFt and state-of-art albumin-conjugated INNO-206 (a DOXO analogue).[23] We wondered whether these favourable bioengineering features of recombinant, modified HFts come at the cost of a reduced interaction with their specific receptor (the transferrin receptor 1, TfR1). This receptor is responsible for highly preferential HFt binding and internalization by many types of tumors cells (i.e. from liver, lung, pancreas, colon, cervix, ovary, prostate, breast, sarcoma, and thymus).[3, 25]

The interactions between immobilized His-tagged TfR1 and its soluble interactors, namely wild-type HFt, HFt-PAS40 and HFt-PAS75, bearing PAS shielding polymers of different length, were measured by SPR on a Biacore X100 instrument (see Fig. 2). In the tested range of analyte concentrations the interaction of TfR1 with wild-type HFt fits a 1:1 binding model (Fig. 2, panel A). The corresponding kinetic parameters are reported in Table I. An apparent K_D value of $9.5 \pm 0.3 \text{ nM}$ was estimated. This is the first reported quantitative affinity measurement since the discovery of the interaction between wild-type HFt and TfR1.[22] As expected, at higher analyte concentrations sensorgrams deviate from a single exponential curve, both in the association and

dissociation processes, likely due to formation of ferritin oligomers. These display lower number of apparent binding sites, and hence reduced binding affinity for TfR1. This heterogeneity in analyte binding negligibly affects the dissociation constant, as it remains below 10% of the overall signal amplitude at all tested analyte concentrations. When SPR measurements were carried out with HFt-PAS40 and HFt-PAS75 signal amplitude was reduced and k_{on} and k_{off} parameters varied (Fig. 2, panels B and C, Table II), resulting in K_D value of 53 ± 2 nM and 54 ± 1 nM, respectively. Affinity decrease was accompanied by the enhancement of analyte fraction that deviates from a simple 1:1 binding model. Thus, PAS tails cause a change in sensorgram amplitude, apparently heterogeneous ligand:analyte stoichiometry and significant drop in affinity, but do not abolish HFt NPs ability to bind the TfR1 receptor.

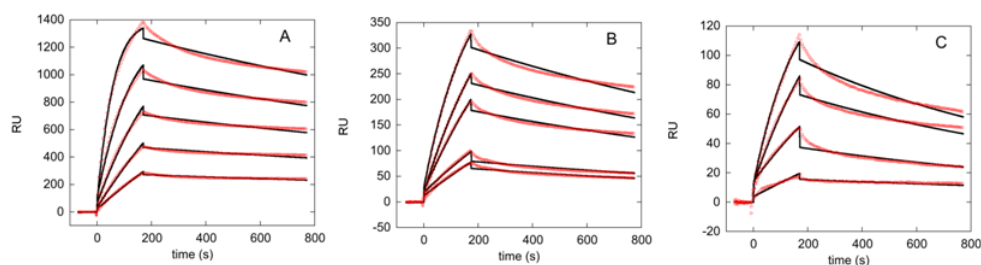


Fig. 2. Sensorgrams of the interaction between immobilized His-tagged TfR1 and HFt-based NPs (soluble analytes). Experimental data at increasing analyte concentrations are shown in red, whereas ideal fits to a 1:1 binding model are reported as black lines, as a reference. Wild-type HFt and HFt-PAS40 were used at 0.5, 0.25, 0.125, 0.0625 and 0.03125 μ M concentrations in panels A and B, respectively. HFt-PAS75 was used at 0.45, 0.225, 0.112, and 0.028 μ M in panel C. RU, resonance units.

TABLE II. Kinetic parameters for SPR experiments

Protein analyte	k_{on} ($M^{-1} s^{-1}$)	k_{off} (s^{-1})	K_D (nM)
HFt	$(4.39 \pm 0.09) \times 10^4$	$(4.19 \pm 0.04) \times 10^{-4}$	9.5 ± 0.3
HFt-PAS40	$(1.07 \pm 0.03) \times 10^4$	$(5.73 \pm 0.03) \times 10^{-4}$	53 ± 2
HFt-PAS75	$(1.90 \pm 0.03) \times 10^4$	$(1.03 \pm 0.01) \times 10^{-3}$	54 ± 1

3.2. Design and production of novel HFt-MP-PAS40 and HFt-MP-PAS75 containing an MMP-cleavable site

Far from hampering *in vivo* biotechnological application, the observed reduction in binding affinity of PASylated constructs may even turn useful. On the one hand, it may reduce off-target delivery to healthy cells, since in these the TfR1 receptor is expressed at such low levels that a drop in binding affinity may act as an additional rate limiting step and barrier to PASylated HFt uptake. Hence, payload accumulation in normal tissues and the half life of PASylated constructs in the circulation may be reduced and enhanced, respectively, favouring recirculation to the tumor site. These predictions are in line with previous observations of ours demonstrating longer half-lives of HFt-PAS40 and HFt-PAS75 in the bloodstream.[23]

Yet, one may argue that although tumors express high levels of TfR1, some adverse effects of low affinity binding are expected.

To compensate for potential TfR1 affinity reduction due to PASylation, the PLGLAG hexapeptide was incorporated in recombinant HFt constructs between HFt core and PAS shell. This peptide is a substrate of tumor proteinases MMP-2 and MMP-9, which cleave it at GL site and are enriched in the tumor microenvironment.[26] This strategy makes HFt-PAS constructs responsive to tumor-selective stimuli, which are expected to remove moieties interfering with TfR1 binding. Fusion proteins HFt-MP-PAS40 and HFt-MP-PAS75 were obtained via recombinant protein technology and successfully purified at high yields (100 mg per *E. coli* litre) as soluble fractions of *E. coli* growth. Importantly, both constructs retained biophysical features identical to those of the parent HFt-PAS40 and HFt-PAS75 proteins: spontaneous assembly into 24-meric oligomers, high solubility in both buffer and plasma, and excellent DOXO encapsulation ability (Fig. S-1).

3.3. Removal of PAS shields from HFt-based NPs in the presence of MMP2/9 proteinases

HFt-MP-PAS75 was mixed with collagenase IV (containing MMP-2 and 9) in solution and incubated at 37°C for two hours. Then, samples were analyzed by SEC gel chromatography and SDS-PAGE. Fig. 3A shows typical size-exclusion chromatography profiles of HFt-MP-PAS75 before and after PAS removal, with two clearly separated elution peaks. In SDS-PAGE the HFt core released by MMP-2/9-mediated cleavage migrates to essentially the same gel position as wild-type HFt and leaves no detectable band at the MP-PAS75 position (Fig. 3B). The efficacy of PAS removal formally demonstrates that even the longest PAS polymers used in our constructs do not mask the MMP cleavage site. Similar results were obtained for HFt-MP-PAS40 (Figure S-2).

Importantly, the HFt core released by PAS removal had wild-type like TfR1 binding properties. SPR analysis revealed that TfR1 binding affinity (apparent K_D) is in the 10 nM range, a value superimposable to that of wild-type HFt.

These results demonstrate that a fully functional HFt core is recovered at the end of a complex process involving synthesis, assembly and proteolytic cleavage.

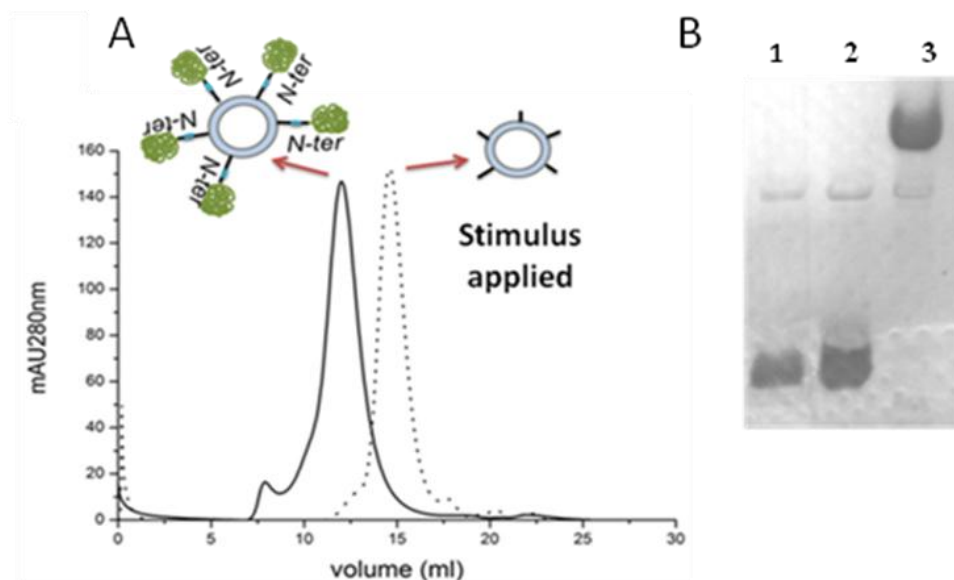


Fig. 3. HFt-MP-PAS75 PAS shield removal *in vitro*. (A) SEC profiles of HFt-MP-PAS75 before (solid line) and after (dotted line) PAS sequence removal by MMP-2/9 proteinase *in vitro*. (B) SDS-PAGE band migration profiles of MP-PAS75 before and after PAS removal. *Lane 1* HFt (1 mg/ml); *Lane 2*, HFt-MP-PAS75 (2 mg/ml) after *in vitro* digestion with 0.5 mg/ml MMP-2/9 proteinases; *Lane 3*, HFt-MP-PAS75 (2 mg/ml). SDS-PAGE was stained with Coomassie brilliant blue R-250.

3.4. Binding of HFt-MP-PAS-DOXO NPs to tumor cell lines

Our previously reported disassembly/reassembly method (see experimental section) was employed to encapsulate about 90 DOXO molecules inside the cavity of HFt-MP-PAS40 (HFt-MP-PAS40-DOXO) and HFt-PAS40 (HFt-PAS40-DOXO), containing and lacking the MMP cleavage site, respectively.[23] The ability of the two NPs to bind HT1080 sarcoma or PaCa-44 pancreatic cancer cells was assessed in parallel by flow cytometry (FACS), taking advantage of DOXO fluorescent emission in the FL2-PE channel. Experiments were carried out at the

temperature values of 37°C (uptake) or 4°C (binding), at which MMPs are expected to be enzymatically active and inactive, respectively. As shown in Fig. 4, at 4°C median fluorescence intensity (MFI) values of HFt-PAS40-DOXO and HFt-MP-PAS40-DOXO for HT1080 cells were low and comparable. Conversely, at 37°C MFI of HFt-MP-PAS40-DOXO was about 4-fold higher whereas HFt-PAS40-DOXO binding did not significantly increase. Similar results were obtained for PaCa44 cells, although differences after 1 hour of incubation are less evident and become more significant after 3-5 hours (Figure S-3). These differences may be ascribed to lower levels of MMPs activity in PaCa44 cells compared with HT1080 cells.

In agreement with SPR and *in vitro* cleavage assays, these results indicate that HFt-NPs binding to cancer cells is significantly reduced by the presence of the PAS tail and restored following MMP site cleavage. Similar results were obtained using analogous HFt-PAS75-DOXO and HFt-MP-PAS75-DOXO constructs (data not shown).

Therefore, the HFt-MP-PAS40/75-DOXO NPs thus obtained are endowed with both long circulation half-life properties and tumor-stimuli dependent high affinity binding.

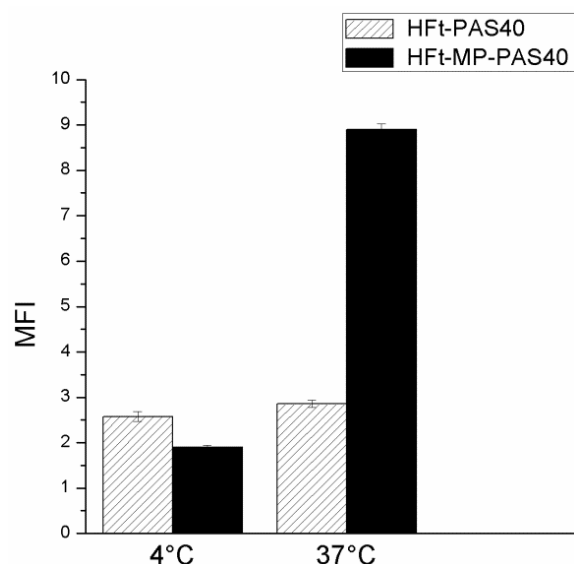


Fig. 4. PAS shield removal in sarcoma cell culture. Flow cytometric analysis of HFt-based NPs. DOXO-containing HFt-PAS40 and HFt-MP-PAS40 preparations were incubated for 1 h at 4°C or 37°C with human HT-1088 cells. Binding was revealed by direct fluorescence reading in a CyAN ADP flow cytometer. HFt-based NPs were provided at the predetermined optimal concentration of 0.15 mg/ml (in protein). MFI refers to the median fluorescence intensity of the sample divided to cell autofluorescence.

3.5. Sub-cellular localization of HFt-based NPs

To determine whether HFt-MP-PAS-DOXO NPs undergo cell surface binding *versus* uptake and internalization, the intracellular localization of these compounds was investigated by incubating them in HT-1088 cells at 37°C for 20 min or 3 h and visualizing DOXO-associated fluorescence by confocal microscopy.

The results obtained with HFt-MP-PAS40-DOXO and HFt-MP-PAS75-DOXO were very similar. Remarkably, internalization was very rapid and involved massive DOXO translocation into the nuclei. Nuclear localization was already evident after 20 min incubation (Figure S-4), and steadily increased thereafter. At 3h, DOXO localization to the nucleus was extremely evident for both constructs (Fig. 5).

Nuclear dispatch of these HFt-based NPs does not match the natural intracellular routing of drug-free HFt, which preferentially localizes to cytoplasm and lysosomes, but is very similar to the results reported by two groups using HFt-DOXO complexes.[7, 27] Authors suggested that following TfR1 binding at cell surface, HFt-DOXO is internalized in an endosomal compartment where a mildly acidic (pH 5.5) favours some DOXO release/translocation in the cytoplasm, diffusion to the nucleus and initial DNA damage. DOXO would then trigger a self-sustained, progressive nuclear translocation loop leading to extensive cell damage.[7, 27] Likewise, our HFt-based NPs are likely to act like "Trojan horses" delivering high amounts of the drug right to the site of action of the drug itself. As a consequence, speed and efficiency of nuclear delivery of the here reported HFt-based NPs greatly outperform those of albumin-DOXO conjugates (i.e. INNO-206), which result in DOXO accumulation mainly in the cytoplasm.[28]

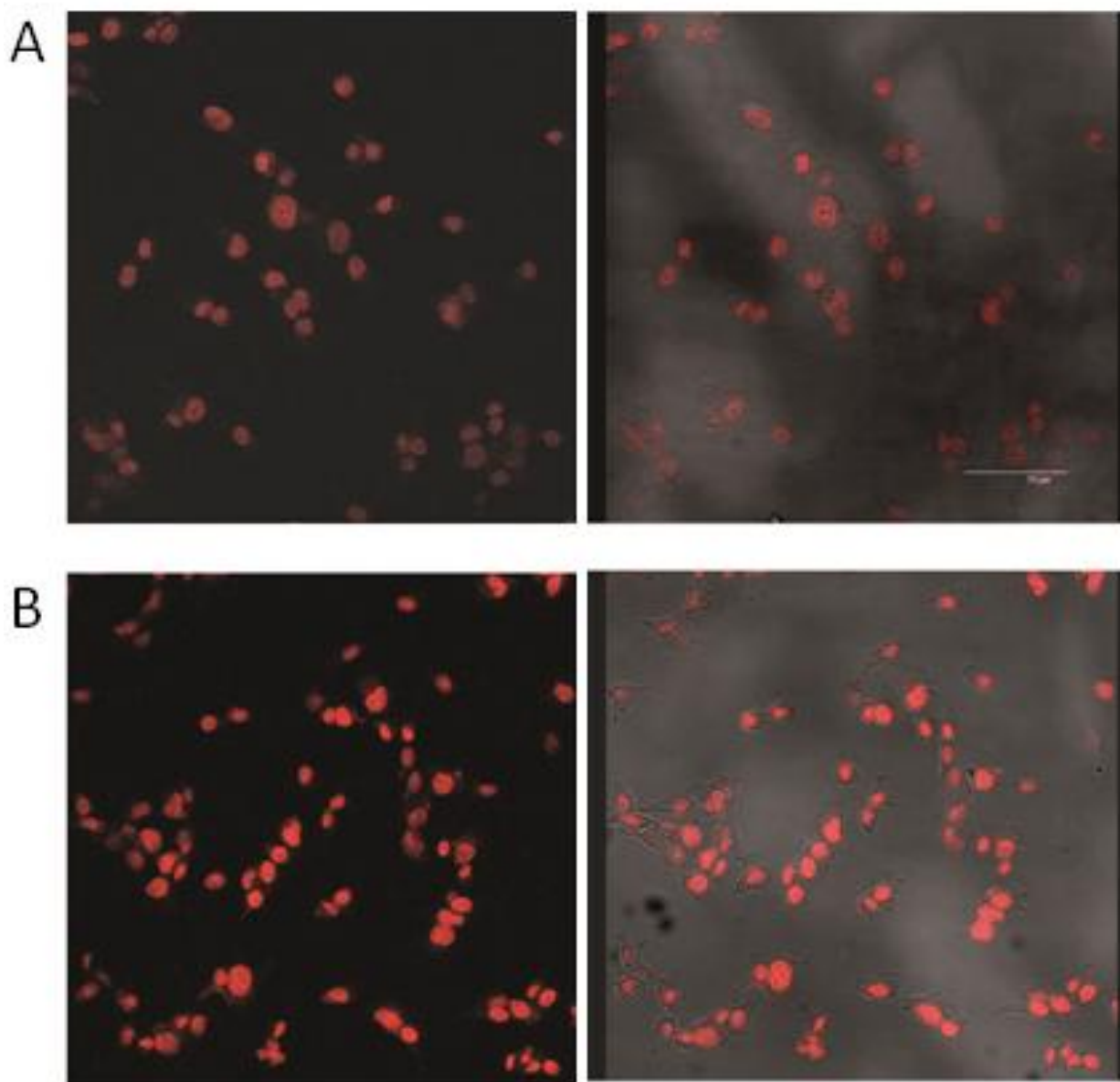


Fig. 5. Representative confocal microscopy images obtained after 3 h incubation of HT1080 cells with 0.25 mg/ml HFt-MP-PAS40-DOXO (A) and HFt-MP-PAS75-DOXO (B). Left: images in the PE channel, DOXO fluorescence (red). Right: merge of fluorescence and light transmission cell images.

3.6. *In vitro* antiproliferative effects of HFt-based NPs

To assess the ability of DOXO-loaded HFt-based NPs to intoxicate and to kill cancer cells *in vitro* we performed XTT assays on human fibrosarcoma HT1080 and human pancreatic cancer

PaCa-44 cells. Both cell lineages exemplify tumor histotypes extremely refractory to conventional chemotherapeutic drugs.[29] As reported in Table 2, HFt-MP-PAS40-DOXO and HFt-MP-PAS75-DOXO IC₅₀ values were similar to those of naked DOXO in both cell lines. This is remarkable, since in cell culture systems naked drugs freely diffuse into cells, whereas HFt-NPs deliver DOXO by rate-limiting receptor-mediated uptake.

Table 2. IC₅₀ values of DOXO, HFt-MP-PAS40-DOXO and HFt-MP-PAS75-DOXO treatment of human cell lines PaCa-44 (pancreatic carcinoma) and HT1080 (fibrosarcoma). Mean ± S.D values of 3 independent experiments are reported.

Treatment¹	IC₅₀ (μM)	IC₅₀ (μM)
	<i>PaCa-44</i>	<i>HT1080</i>
DOXO	0.15 ± 0.03	0.02 ± 0.03
HFt-MP-PAS40-DOXO	0.11 ± 0.03	0.07 ± 0.04
HFt-MP-PAS75-DOXO	0.05 ± 0.002	0.08 ± 0.03

¹ 96 h (48 + 48 h)

3.7. Therapeutic efficacy of HFt-based NPs *in vivo*

To evaluate *in vivo* chemotherapeutic efficacy of receptor-uptaken, DOXO-encapsulating HFt-NPs we treated nude mice bearing xenogeneic PaCa-44 tumor. To compare results with state-of-art treatments, mice were treated in parallel with normalized dosages of the novel DOXO prodrug formulation INNO-206. INNO-206 is a (6-maleimidocaproyl) hydrazone DOXO derivative that, following systemic injection, electively reacts with cysteine 34 of serum albumin forming an acid-cleavable bond. Once the albumin-bound form reaches its final tissue destination, the drug is released. INNO-206 has been reported to have superior antitumor efficacy and lower toxic effects than DOXO in animal models.[30-31] In 2012, INNO-206 has been granted orphan drug designation by the U.S. Food and Drug Administration (FDA) for the treatment of patients with pancreatic cancer. Phase 2 proof-of-concept clinical trials are ongoing in patients with pancreatic cancer, small cell lung cancer and glioblastoma. Soft tissue sarcoma studies reached Phase 3. In patients as well, adverse events and efficacy of INNO-206 are reported to be

significantly reduced and enhanced, respectively, as compared with DOXO, making INNO-206 a particularly pertinent control for HFt-based NPs.[32]

In a first experiment, INNO-206, HFt-MP-PAS40-DOXO, HFt-MP-PAS75-DOXO or PBS were injected i.v. twice a week for two weeks into mice bearing tumor masses of about 100 mm³. Pancreas carcinoma tumors with this size typically display Gompertzian kinetics,[33] and are in logarithmic growth phase, with new tumor vessels robustly developing and absence of necrosis in the tumor interior. DOXO doses of 5 mg/Kg were used, which are slightly below the reported maximum tolerated dose (MTD: about 6-7 mg/Kg). In PBS-treated groups tumors grew rapidly to reach an average volume of ≥ 1000 mm³ on day 24 after tumor cell injection, corresponding to the 4th day after the last administered injection (Fig. 6 and Figure S-5A). As expected, INNO-206 treatment significantly reduced tumor growth rate. Importantly, treatment with either HFt-MP-PAS40-DOXO or HFt-MP-PAS75-DOXO determined even larger tumor growth regression and the apparent efficacy exceeded that of INNO-206 by a factor of about 4 (Fig. 6 and Figure S-5A).

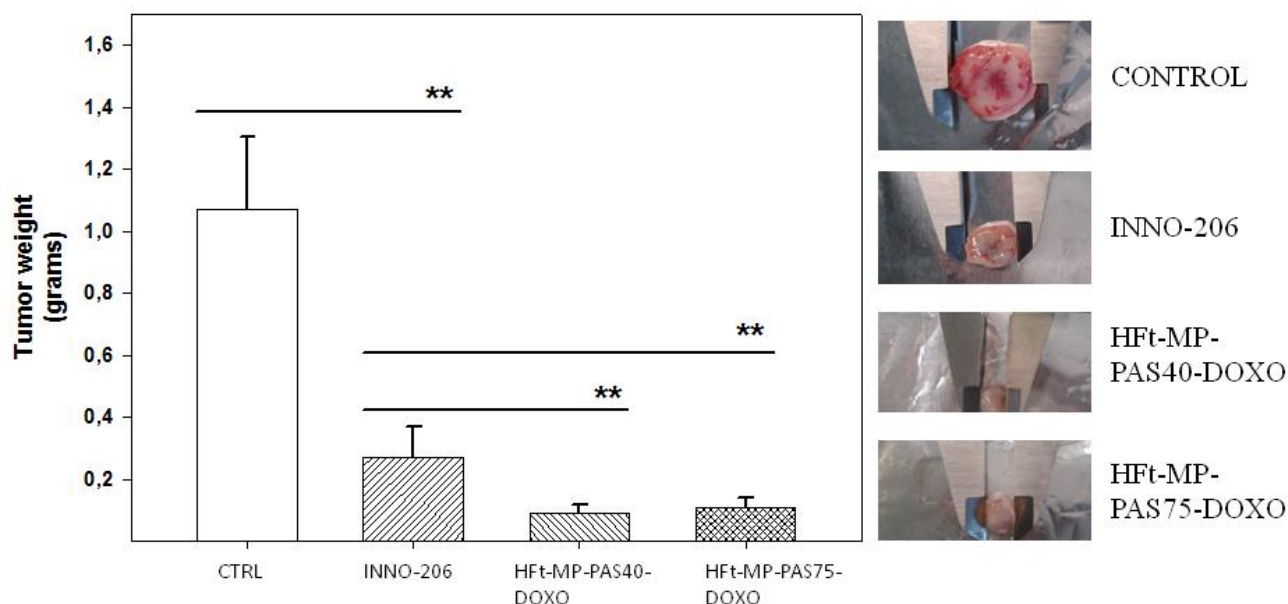
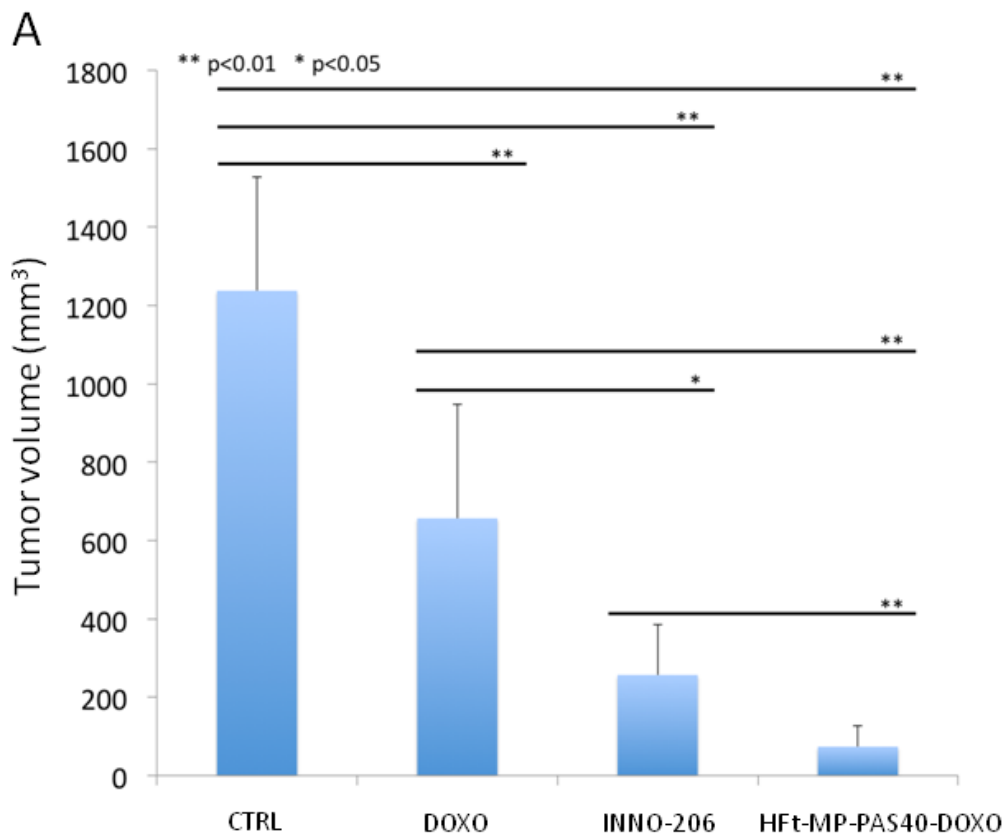


Fig. 6. Anti-tumor activity of DOXO-containing HFt-based NPs. PaCa-44 tumor cells were injected s.c. into nude mice. When tumors reached about 100 mm³ volume mice were treated with INNO-206, HFt-MP-PAS40-DOXO, HFt-MP-PAS75-DOXO or PBS. Treatments were normalized according to DOXO dose (i.e., 5 mg/kg DOXO in all preparations). Left panel: Tumor weights at sacrifice. Bars represent means \pm SD, n = 5, **p<0.01. Right panel: Representative images of the tumor mass at the end of the experiment.

Mice were monitored for body weight and signs of distress as well. No abnormal behaviour or appreciable body weight loss were observed in mice treated with HFt-MP-PAS40-DOXO (Figure S-5B). In contrast, mice receiving MP-PAS-75-DOXO at the same concentration exhibited about 15% weight loss. For this reason, and because of the slightly higher efficacy with respect to the PAS75-containing construct, we focussed on HFt-MP-PAS40-DOXO in a subsequent experiment aimed at evaluating long-term survival. In this experiment, we also included naked DOXO and INNO-206 for comparison purposes.



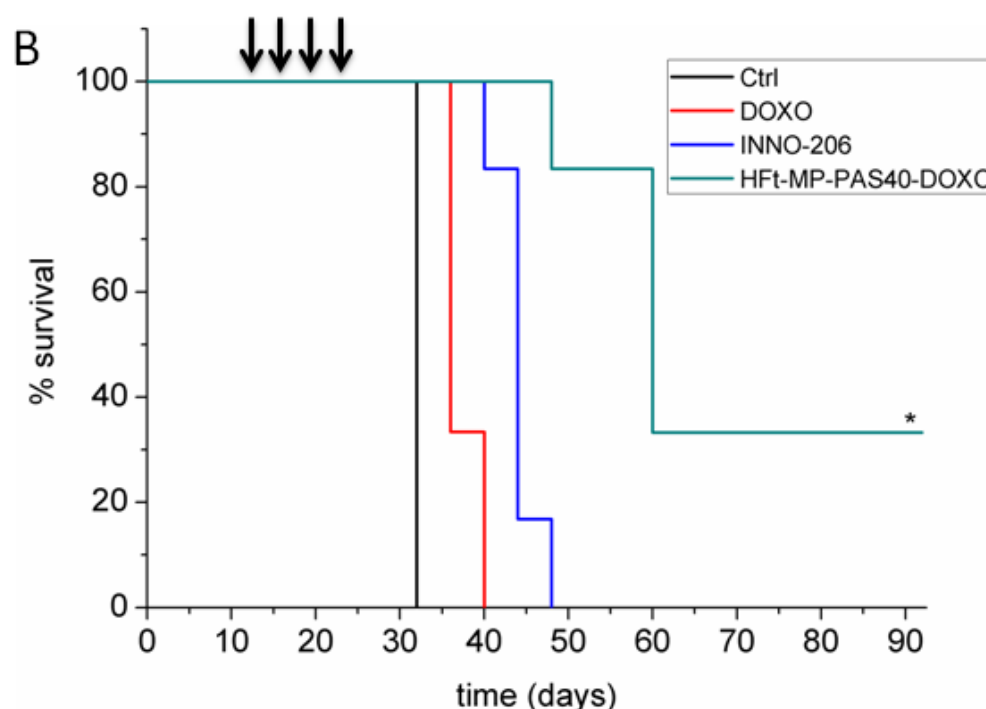


Fig. 7. Anti-tumor activity of HFt-MP-PAS40-DOXO. PaCa-44 tumor cells were injected s.c. into nude mice. When tumors reached about 100 mm³ volume mice were i.v. treated with DOXO, INNO-206, HFt-MP-PAS40-DOXO or PBS. (A) Tumor volumes for mice groups 32 days after tumor cell injection. (B) Survival curves of different animal groups; mice were sacrificed when the tumor had reached a volume ≥ 1000 mm³. Arrows indicate the four days cycle of administration of each of the four treatments (5 mg/kg DOXO equivalents). Bars represent means \pm SD, n = 6.

In agreement with the previous experiment, HFt-MP-PAS40-DOXO reduced tumor size about 4 and 8 times more efficiently than INNO-206 and DOXO, respectively (Fig. 7A). Treatment with naked DOXO offered limited survival benefit compared to negative controls (Fig. 7B). Mice treated with INNO-206 had 12 day longer median survival times. However, neither DOXO nor INNO-206 were able to induce stall in tumor growth after four administration cycles. In contrast, complete blockade of tumor growth associated with partial remission was obtained in mice treated with four cycles of HFt-MP-PAS40-DOXO. Strikingly, 33% of mice were still alive after 90 days (Fig. 7B). The remaining 67% mice treated with HFt-MP-PAS40-DOXO were sacrificed, according to ethical guidelines, based on a tumor volume ≥ 1000 mm³. However, 50% of sacrificed mice had highly colliquated tumor masses, suggesting that the survival time of HFt-MP-PAS40-DOXO had been underestimated.

4. Conclusions

We have designed and developed two novel HfT-based, PAS-bearing, DOXO-loaded constructs characterized by the following features: (a) outer PAS shells of different sizes; and (b) stimuli-sensitive/tumor-selective sequence responsive to proteolytic cleavage by MMPs. Both HfT-based NPs are expressed in high yields in *E. coli*; self-assemble into a wild-type like 24meric NP; are highly stable in both laboratory buffers and mouse plasma; encapsulate stably up to 90 DOXO molecules in the internal cavity. The design had the following aims. Following administration, PAS polymers are expected to shield the HfT core from, and reduce binding affinity for, the TfR1 receptor, expressed at low levels by normal tissues, thus reducing off-target dispatch and unwanted toxicity and allowing longer permanence in the bloodstream. At the tumor level, the PAS shield can be removed by tumor-specific proteases restoring HfT affinity for TfR1 and intracellular uptake, which result in on-site toxicity. *In vitro* assay demonstrated that DOXO-loaded HfT-based NPs inhibited tumor cell proliferation with an efficacy superimposable to the free drug DOXO. It is noteworthy to mention that Abraxane[®], a paclitaxel-loaded albumin nanosystem, currently approved for the treatment of metastatic breast carcinoma showed the same killing efficacy as the naked paclitaxel *in vitro*. [34] In addition, INNO-206, the DOXO-containing albumin nanosystem, was reported to have a much lower efficacy than the naked DOXO against lung and pancreatic cancer cells *in vitro*, with IC₅₀ values up to 13 and 19 times higher than DOXO, respectively. [28, 30]

Strikingly, our constructs displayed excellent therapeutic efficacy in a human pancreatic cancer model *in vivo*, increasing animal overall survivals significantly. Here, their efficacy was significantly superior even to the novel albumin-based DOXO delivery system (INNO-206), which is currently in phase III clinical trials. Interestingly, INNO-206 has been shown to mainly deliver DOXO and its analogues to the cytoplasm, [28] and does not have any known ability to hijack the endocytosis machinery for nuclear translocation. Therefore the higher *in vivo* efficacy of our nanosystems could also be ascribable to the increased delivery into the nucleus as observed in the confocal microscopy studies.

All the above findings provide solid evidence indicating that stimuli-sensitive HfT-based NPs could be considered first-in-class platforms for chemotherapeutic delivery. HfT-MP-PAS NPs are fully recombinant constructs that do not require *ad hoc* manipulations, coupling steps, and/or

separation procedures after synthesis. The *in vitro* and *in vivo* properties of DOXO-loaded constructs fully justify carrying out additional preclinical studies to assess the possibility to exploit their selective cancer killing properties in cancer therapy.

Acknowledgements

The present work is dedicated to Matilde Pizzocaro, who recently and prematurely passed away. This research was supported by grants from the MIUR flagship Project "Nanomax" (A.B.), Associazione Italiana per la Ricerca sul Cancro (AIRC) I.G. Grant 14204 (P.G.) and I.G. Grant 16776 (P.C.). G.F. gratefully acknowledges Fondazione Cariverona, Verona Nanomedicine Initiative and Italian Minister of Health RF-2010-2305526 for supporting this work. P.C., G.D. and S.A. gratefully acknowledge the Pizzocaro family for their grant support.

Appendix A. Supplementary data

Supplementary data to this article can be found online at <http://>

REFERENCES

- [1] E. Falvo, E. Tremante, R. Fraioli, C. Leonetti, C. Zamparelli, A. Boffi, V. Morea, P. Ceci, P. Giacomini, Antibody-drug conjugates: targeting melanoma with cisplatin encapsulated in protein-cage nanoparticles based on human ferritin, *Nanoscale*, 5 (2013) 12278-12285.
- [2] Z. Zhen, W. Tang, H. Chen, X. Lin, T. Todd, G. Wang, T. Cowger, X. Chen, J. Xie, RGD-Modified Apoferritin Nanoparticles for Efficient Drug Delivery to Tumors, *Acs Nano*, 7 (2013) 4830-4837.
- [3] K. Fan, C. Cao, Y. Pan, D. Lu, D. Yang, J. Feng, L. Song, M. Liang, X. Yan, Magnetoferritin nanoparticles for targeting and visualizing tumour tissues, *Nat Nanotechnol*, 7 (2012) 459-464.
- [4] L. Vannucci, E. Falvo, M. Fornara, P. Di Micco, O. Benada, J. Krizan, J. Svoboda, K. Hulikova-Capkova, V. Morea, A. Boffi, P. Ceci, Selective targeting of melanoma by PEG-masked protein-based multifunctional nanoparticles, *Int J Nanomedicine*, 7 (2012) 1489-1509.
- [5] L. Vannucci, E. Falvo, C.M. Failla, M. Carbo, M. Fornara, R. Canese, S. Cecchetti, L. Rajsiglova, D. Stakheev, J. Krizan, A. Boffi, G. Carpinelli, V. Morea, P. Ceci, In Vivo Targeting of Cutaneous Melanoma Using an Melanoma Stimulating Hormone-Engineered Human Protein Cage with Fluorophore and Magnetic Resonance Imaging Tracers, *Journal of Biomedical Nanotechnology*, 11 (2015) 81-92.
- [6] M. Liang, K. Fan, M. Zhou, D. Duan, J. Zheng, D. Yang, J. Feng, X. Yan, H-ferritin-nanocaged doxorubicin nanoparticles specifically target and kill tumors with a single-dose injection, *Proc Natl Acad Sci U S A*, 111 (2014) 14900-14905.
- [7] M. Bellini, S. Mazzucchelli, E. Galbiati, S. Sommaruga, L. Fiandra, M. Truffi, M.A. Rizzuto, M. Colombo, P. Tortora, F. Corsi, D. Prospero, Protein nanocages for self-triggered nuclear delivery of DNA-targeted chemotherapeutics in Cancer Cells, *J Control Release*, 196 (2014) 184-196.
- [8] Z. Heger, S. Skalickova, O. Zitka, V. Adam, R. Kizek, Apoferritin applications in nanomedicine, *Nanomedicine-Uk*, 9 (2014) 2233-2245.

- [9] G. Bellapadrona, S. Sinkar, H. Sabanay, V. Liljestrom, M. Kostianen, M. Elbaum, Supramolecular Assembly and Coalescence of Ferritin Cages Driven by Designed Protein-Protein Interactions, *Biomacromolecules*, 16 (2015) 2006-2011.
- [10] Y.J. Kang, D.C. Park, H.H. Shin, J. Park, S. Kang, Incorporation of Thrombin Cleavage Peptide into a Protein Cage for Constructing a Protease-Responsive Multifunctional Delivery Nanoplatform, *Biomacromolecules*, 13 (2012) 4057-4064.
- [11] L. Schoonen, J.C. van Hest, Functionalization of protein-based nanocages for drug delivery applications, *Nanoscale*, 6 (2014) 7124-7141.
- [12] M. Truffi, L. Fiandra, L. Sorrentino, M. Monieri, F. Corsi, S. Mazzucchelli, Ferritin nanocages: A biological platform for drug delivery, imaging and theranostics in cancer, *Pharmacol Res*, 107 (2016) 57-65.
- [13] J.H. Lee, H.S. Seo, J.A. Song, K.C. Kwon, E.J. Lee, H.J. Kim, E.B. Lee, Y.J. Cha, J. Lee, Proteinticle engineering for accurate 3D diagnosis, *Acs Nano*, 7 (2013) 10879-10886.
- [14] E.J. Lee, N.K. Lee, I.S. Kim, Bioengineered protein-based nanocage for drug delivery, *Adv Drug Deliv Rev*, (2016).
- [15] L. Li, L. Zhang, M. Knez, Comparison of Two Endogenous Delivery Agents in Cancer Therapy: Exosomes and Ferritin, *Pharmacol Res*, (2016).
- [16] M. Uchida, D.A. Willits, K. Muller, A.F. Willis, L. Jackiw, M. Jutila, M.J. Young, A.E. Porter, T. Douglas, Intracellular Distribution of Macrophage Targeting Ferritin-Iron Oxide Nanocomposite, *Adv Mater*, 21 (2009) 458-462.
- [17] S.G. Crich, B. Bussolati, L. Tei, C. Grange, G. Esposito, S. Lanzardo, G. Camussi, S. Aime, Magnetic resonance visualization of tumor angiogenesis by targeting neural cell adhesion molecules with the highly sensitive gadolinium-loaded apoferritin probe, *Cancer Research*, 66 (2006) 9196-9201.
- [18] X. Lin, J. Xie, G. Niu, F. Zhang, H. Gao, M. Yang, Q. Quan, M.A. Aronova, G. Zhang, S. Lee, R. Leapman, X. Chen, Chimeric ferritin nanocages for multiple function loading and multimodal imaging, *Nano Lett*, 11 (2011) 814-819.
- [19] E. Fantechi, C. Innocenti, M. Zanardelli, M. Fittipaldi, E. Falvo, M. Carbo, V. Shullani, L. Di Cesare Mannelli, C. Ghelardini, A.M. Ferretti, A. Ponti, C. Sangregorio, P. Ceci, A smart platform for hyperthermia application in cancer treatment: cobalt-doped ferrite nanoparticles mineralized in human ferritin cages, *Acs Nano*, 8 (2014) 4705-4719.
- [20] X.Y. Liu, W. Wei, S.J. Huang, S.S. Lin, X. Zhang, C.M. Zhang, Y.G. Du, G.H. Ma, M. Li, S. Mann, D. Ma, Bio-inspired protein-gold nanoconstruct with core-void-shell structure: beyond a chemo drug carrier, *J Mater Chem B*, 1 (2013) 3136-3143.
- [21] S.A. Bode, I.J. Minten, R.J. Nolte, J.J. Cornelissen, Reactions inside nanoscale protein cages, *Nanoscale*, 3 (2011) 2376-2389.
- [22] L. Li, C.J. Fang, J.C. Ryan, E.C. Niemi, J.A. Lebron, P.J. Bjorkman, H. Arase, F.M. Torti, S.V. Torti, M.C. Nakamura, W.E. Seaman, Binding and uptake of H-ferritin are mediated by human transferrin receptor-1, *Proc Natl Acad Sci U S A*, 107 (2010) 3505-3510.
- [23] E. Falvo, E. Tremante, A. Arcovito, M. Papi, N. Elad, A. Boffi, V. Morea, G. Conti, G. Toffoli, G. Fracasso, P. Giacomini, P. Ceci, Improved Doxorubicin Encapsulation and Pharmacokinetics of Ferritin-Fusion Protein Nanocarriers Bearing Proline, Serine, and Alanine Elements, *Biomacromolecules*, (2015).
- [24] J.E. Rundhaug, Matrix metalloproteinases, angiogenesis, and cancer: commentary re: A. C. Lockhart et al., Reduction of wound angiogenesis in patients treated with BMS-275291, a broad spectrum matrix metalloproteinase inhibitor. *Clin. Cancer Res.*, 9: 00-00, 2003, *Clin Cancer Res*, 9 (2003) 551-554.
- [25] K. Fan, L. Gao, X. Yan, Human ferritin for tumor detection and therapy, *Wiley Interdiscip Rev Nanomed Nanobiotechnol*, 5 (2013) 287-298.
- [26] N.Q. Shi, W. Gao, B. Xiang, X.R. Qi, Enhancing cellular uptake of activable cell-penetrating peptide-doxorubicin conjugate by enzymatic cleavage, *Int J Nanomedicine*, 7 (2012) 1613-1621.
- [27] L.B. Zhang, L. Li, A. Di Penta, U. Carmona, F. Yang, R. Schops, M. Brandsch, J.L. Zugaza, M. Knez, H-Chain Ferritin: A Natural Nuclei Targeting and Bioactive Delivery Nanovector, *Adv Healthc Mater*, 4 (2015) 1305-1310.
- [28] U. Beyer, B. Rothen-Rutishauser, C. Unger, H. Wunderli-Allenspach, F. Kratz, Differences in the intracellular distribution of acid-sensitive doxorubicin-protein conjugates in comparison to free and liposomal formulated doxorubicin as shown by confocal microscopy. (vol 18, pg 29, 2001), *Pharm Res-Dordr*, 18 (2001) 719-719.
- [29] P. Monti, F. Marchesi, M. Reni, A. Mercalli, V. Sordi, A. Zerbi, G. Balzano, V. Di Carlo, P. Allavena, L. Piemonti, A comprehensive in vitro characterization of pancreatic ductal carcinoma cell line biological behavior and its correlation with the structural and genetic profile, *Virchows Arch*, 445 (2004) 236-247.

- [30] F. Kratz, S. Azab, R. Zeisig, I. Fichtner, A. Warnecke, Evaluation of combination therapy schedules of doxorubicin and an acid-sensitive albumin-binding prodrug of doxorubicin in the MIA PaCa-2 pancreatic xenograft model, *Int J Pharm*, 441 (2013) 499-506.
- [31] F. Kratz, I. Fichtner, R. Graeser, Combination therapy with the albumin-binding prodrug of doxorubicin (INNO-206) and doxorubicin achieves complete remissions and improves tolerability in an ovarian A2780 xenograft model, *Invest New Drugs*, 30 (2012) 1743-1749.
- [32] C. Unger, B. Haring, M. Medinger, J. Dreves, S. Steinbild, F. Kratz, K. Mross, Phase I and pharmacokinetic study of the (6-maleimidocaproyl)hydrazone derivative of doxorubicin, *Clin Cancer Res*, 13 (2007) 4858-4866.
- [33] L. Norton, R. Simon, H.D. Brereton, A.E. Bogden, Predicting the course of Gompertzian growth, *Nature*, 264 (1976) 542-545.
- [34] E. Bernabeu, G. Helguera, M.J. Legaspi, L. Gonzalez, C. Hocht, C. Taira, D.A. Chiappetta, Paclitaxel-loaded PCL-TPGS nanoparticles: in vitro and in vivo performance compared with Abraxane(R), *Colloids Surf B Biointerfaces*, 113 (2014) 43-50.

Supplementary Material

[Click here to download Supplementary Material: supplementary material_Fracasso et al.docx](#)